2010 American Control Conference
Marriott Waterfront, Baltimore, MD, USA
June 30-July 02, 2010

Nonlinear Observer for Structure Estimation using a Paracatadioptric Camera

Ashwin P. Dani, Nicholas R. Fischer, Zhen Kan, Warren E. Dixon

Abstract— **Estimation of the three-dimensional (3D) Euclidean coordinates of points on an object using two-dimensional (2D) image data is required by many robotics and surveillance applications. This paper develops a nonlinear observer to estimate relative Euclidean coordinates of an object viewed by a moving paracatadioptric camera with known motion. The observer exponentially estimates the structure of an object (i.e. Euclidean coordinates of different points on an object) provided sufficient observability conditions are satisfied. Observer gain conditions are derived based on a Lyapunov-analysis, which guarantees convergence, and simulation results illustrate the performance of the observer in the presence of image noise.**

I. Introduction

Numerous contemporary applications use (or would benefit from using) feedback from a camera to provide properly scaled Euclidean information about a static three-dimensional (3D) scene. Some information about the structure of the scene can be determined from the camera moving with a known trajectory, yet the fundamental challenge is to inject some Euclidean measure in the scene so the Euclidean coordinates of targets can be properly scaled. This challenge is due to the loss of depth information (i.e., the distance from the camera to the target) for the 3D scene through the projection to two-dimensional (2D) images. If the depth information can be determined with proper scale, then the image coordinates of feature points can be used to reconstruct the 3D structure of the scene. Estimating the 3D structure from the 2D images formed by a moving camera system, with known camera motion, is the classic "structure from motion (SfM)" problem.

Many solutions have been developed for the SfM problem using a conventional perspective camera (e.g. see [1]–[10]). Solutions to the SfM problem are broadly classified as offline methods (batch methods) or online methods (iterative and feedback methods). Some of the online solutions rely on the use of an Extended Kalman filter (EKF) [7], [11]–[13]. Kalman filter based approaches lack a convergence guarantee and could converge to wrong solutions in practical scenarios. Also, *a priori* knowledge about the noise is required for such solutions. In comparison to Kalman filter-based approaches, some researchers have developed nonlinear observers for SfM with analytical proofs of stability. For example, a discontinuous high-gain observer called the identifier-based observer (IBO) is presented for structure estimation in [6] under the assumption of known camera motion. In [14], a discontinuous sliding-mode observer is developed which guarantees exponential convergence of the states to an arbitrarily small neighborhood, i.e., uniformly ultimately bounded (UUB) result. A continuous observer which guarantees asymptotic structure estimation is presented in [4] under the assumption of known camera motion.

Given the limited field of view by traditional perspective camera systems, catadioptric camera systems have been investigated [15]–[18]. Catadioptric systems uses a combination of mirrors (e.g., ellipsoid, hyperboloid, and paraboloid) and lenses, placed in a particular configuration, to capture a wider FOV. Although the wider FOV of a catadioptric system is an asset, SfM problems are significantly more complicated than using a traditional perspective camera because of the nonlinear distortion by the mirror/lens combination. Yet, various SfM solutions have been developed for catadioptric systems. In [19], a solution to the SfM problem is presented using bundle adjustment techniques. In [20], [21], a bundle adjustment-based method is developed to estimate the structure in long image sequences for central (i.e., configurations with a single focal length) as well as non-central catadioptric systems. A nonlinear optimization-based technique is developed in [22]–[24] to solve the SfM problem for a catadioptric system. However, convergence of such numerical optimization techniques is not guaranteed and analytical proofs of stability are not provided. Moreover, these methods have limited application for real-time purposes. To address the issues of real-time estimation and convergence guarantee, several investigators have developed nonlinear observers for the SfM problem. In [25], a linear approximation-based observer is presented for planar, spherical, and paraboloid imaging surfaces, to estimate the structure for a nonaffine catadioptric system. In [26], a nonlinear observer is constructed to asymptotically identify the structure for a nonaffine paracatadioptric system (i.e., a central catadioptric system with a paraboloid mirror and an orthographic projection camera is called a paracatadioptric system [27]). The work in [26] is extended in [28], to asymptotically estimate structure of the scene with affine motion dynamics for paracatadioptric system.

Building on the related work in [4], [26], [28], the current contribution is the development of a continuous nonlinear observer for a paracatadioptric system with affine motion dynamics that yields an exponential stability result. The development of an exponential observer indicates potentially improved robustness (versus an asymptotic result) and faster convergence results which can be critical in image-based

[1]This research is supported in part by the NSF CAREER award number 0547448, NSF award number 0901491, the Department of Energy, grant number DE-FG04-86NE37967 as part of the DOE University Research Program in Robotics (URPR), ASTREC, and NSF I/UCRC.

[2]The authors are with the Department of Mechanical and Aerospace Engineering, University of Florida, Gainesville, FL 32611-6250, USA. Email: {ashwin31, moooink, kanzhen0322, wdixon}@ufl.edu

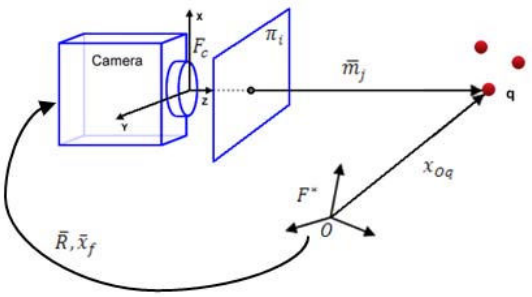

Fig. 1. Moving camera observing a static scene.

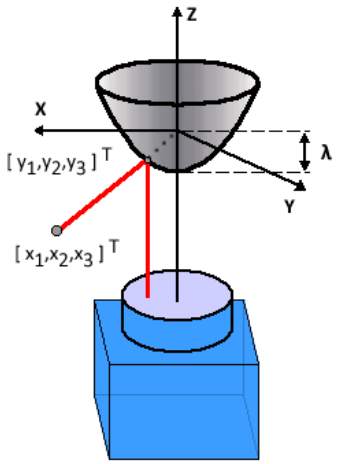

Fig. 2. Omnidirectional camera setup.

applications where the object may only be in the FOV for a limited number of frames. The dynamics of the known states in [28] contain a bounded unmeasurable term and a continuous robust term is used to identify this unmeasurable term. The identified unmeasurable term can be used to estimate the 3D information. In this paper, the state dynamics are reformulated such that the bounded unmeasurable term in [28] can be expressed in terms of an unmeasurable state whose dynamics are represented as a known function of unmeasurable states. This reformulation of the state dynamics allows for the design of an exponentially stable estimator. In the previous work in [28], the known bounds of 3D Euclidean coordinates of a point, camera velocity, acceleration and jerk are required. In the current result, only the bounds on 3D Euclidean coordinates of a point are required to be known. A Lyapunov-based analysis is used to derive an observability condition, which if satisfied, guarantees the estimator converges. Simulation results are provided to demonstrate the performance of the observer with noisy input data.

II. Camera Motion Model

Consider a moving camera viewing a point q on a stationary object. The three dimensional (3D) Euclidean coordinates $\bar{m}(t) \in \mathbb{R}^3$ of the point q in the camera coordinate system are given by

$$\bar{m}(t) \triangleq \begin{bmatrix} x_1(t) & x_2(t) & x_3(t) \end{bmatrix}^T. \tag{1}$$

As the camera is moving, the static point q appears to be moving in the camera reference frame. Let $\mathcal{F}^*$ be an orthogonal coordinate frame attached to the camera at the location corresponding to the time t_0. After the initial time, let an orthogonal coordinate frame attached to the camera be $\mathcal{F}_c$, which has undergone some rotation $\bar{R}(t) \in SO(3)$ and translation $\bar{x}_f(t) \in \mathbb{R}^3$ away from $\mathcal{F}^*$. As seen in Fig. 1, the point q on a static object can be expressed in coordinate system $\mathcal{F}_c$ of the camera as

$$\bar{m} = \bar{x}_f + \bar{R} x_{oq} \tag{2}$$

where x_{oq} is a vector from the origin of coordinate system $\mathcal{F}^*$ to the point q expressed in coordinate system $\mathcal{F}^*$. Differentiating (2) with respect to time, the relative motion of q as observed in the camera coordinate system can be expressed by the following kinematics [9], [29]

$$\dot{\bar{m}} = \begin{bmatrix} a_{11} & a_{12} & a_{13} \\ a_{21} & a_{22} & a_{23} \\ a_{31} & a_{32} & a_{33} \end{bmatrix} \bar{m} + \begin{bmatrix} b_1 \\ b_2 \\ b_3 \end{bmatrix} \tag{3}$$

where $\bar{m}(t)$ is defined in (1), the parameters $a_{ij}(t) \in \mathbb{R}$ $\forall i, j = \{1, 2, 3\}$ of a matrix $A(t) \in \mathbb{R}^{3\times 3}$ denote the rotation parameters and $b(t) = \begin{bmatrix} b_1 & b_2 & b_3 \end{bmatrix}^T \in \mathbb{R}^3$ denotes the linear velocity of the camera. The motion dynamics expressed in (3) represents a general form of object motion describing a rotation, a translation, and a linear deformation [30].

Assumption 1: The linear and angular motion parameters, (i.e. $b(t)$ and $A(t)$) are known bounded functions of time, (i.e. $b(t)$, $A(t) \in \mathcal{L}_\infty$).

III. Geometry of Paracatadioptric Camera

Since the camera is moving, the static point $\bar{m}(t)$ appears to be moving with respect to the camera. Let $\mathcal{F}_m$ be a coordinate system attached to the paraboloid mirror of the paracatadioptric system with the origin of $\mathcal{F}_m$ at the focus of the mirror as shown in Fig. 2. The projection $y(t) = \begin{bmatrix} y_1(t) & y_2(t) & y_3(t) \end{bmatrix}^T \in \mathbb{R}^3$ of the point $\bar{m}(t)$ onto the paraboloid mirror can be expressed as

$$y(t) \triangleq \frac{2\lambda}{L} \begin{bmatrix} x_1(t) & x_2(t) & x_3(t) \end{bmatrix}^T \tag{4}$$

where $\lambda \in \mathbb{R}$ is a known constant that denotes the distance between the focal point and the vertex of the paraboloid mirror, and $L(\bar{m}) \in \mathbb{R}$ is defined as

$$L \triangleq -x_3 + \sqrt{x_1^2 + x_2^2 + x_3^2}. \tag{5}$$

The states $y_1(t)$ and $y_2(t)$ are related to the pixel coordinates in the image, $p = \begin{bmatrix} u & v \end{bmatrix}^T \in \mathbb{R}^2$ by [9]

$$\begin{bmatrix} u \\ v \end{bmatrix} = \begin{bmatrix} 1 & 0 & 0 \\ 0 & 1 & 0 \end{bmatrix} \begin{bmatrix} y_1 \\ y_2 \\ y_3 \end{bmatrix} + \begin{bmatrix} u_0 \\ v_0 \end{bmatrix} \tag{6}$$

where $u_0, v_0 \in \mathbb{R}$ is the the center pixel of the image. If the camera is calibrated, the states $y_1(t)$ and $y_2(t)$ can be recovered from (6). Using the fact that a paraboloid mirror is rotationally symmetric, the state $y_3(t)$ can be computed from $y_1(t)$ and $y_2(t)$ as [18], [27]

$$y_3 = \frac{y_1^2 + y_2^2}{4\lambda} - \lambda. \tag{7}$$

To facilitate the estimation of $\bar{m}(t)$, a new state $y_4(t) \in \mathbb{R}$ is defined as

$$y_4 \triangleq \frac{2\lambda}{L}. \tag{8}$$

From (4) and (8) the following relationship can be developed

$$y = y_4 \bar{m}. \tag{9}$$

Assumption 2: The constant distance between the focal point and the vertex of the paraboloid mirror is upper bounded by a constant and lower bounded by zero as $\bar{\lambda} \geq \lambda > 0$, where $\bar{\lambda}$ denotes a bounding constant. The boundedness of λ implies the focal point is not a vanishing point.

Assumption 3: The parameter $L(\bar{m})$ is upper and lower bounded by constants as $\bar{L} \geq L(\bar{m}) > \underline{L}$, where $\bar{L}$ and $\underline{L}$ denote positive bounding constants. The assumption that $L(\bar{m}) \in \mathcal{L}_\infty$ implies that $y_4(t) \neq 0$ (i.e., the feature point on the object is not a vanishing point). Furthermore, the assumption that $L(\bar{m}) \neq 0$ implies that $y_4(t) \in \mathcal{L}_\infty$ (i.e., the projection of the feature point is not along the optical axis of the camera), and that $x_1(t)$ and $x_2(t)$ are not simultaneously zero (see (5)).

Assumption 4: Since $p(t)$ is an image space coordinate, $p(t) \in \mathcal{L}_\infty$. Thus, (6) and (7) can be used to conclude that $y(t)$ is bounded as

$$\underline{y_1} \leq y_1(t) \leq \bar{y}_1, \quad \underline{y_2} \leq y_2(t) \leq \bar{y}_2, \quad \underline{y_3} \leq y_3(t) \leq \bar{y}_3$$

where $\underline{y_1}$, $\bar{y}_1$, $\underline{y_2}$, $\bar{y}_2$, $\underline{y_3}$ and $\bar{y}_3$ denote bounding constants.

Remark 1: From Assumption 2, 3 and (8), the bounds on $y_4(t)$ can be established as $\underline{y_4} \leq y_4(t) \leq \bar{y}_4$, where $\underline{y_4}$, $\bar{y}_4$ denote known bounding constants.

IV. Structure Estimation by a Catadioptric Camera

A. Structure Estimation Objective

The considered SfM objective is to estimate the Euclidean coordinates $\bar{m}(t)$ of feature points q in a static scene using a moving paracatadioptric camera with known camera velocities $b(t)$ and $\omega(t)$. Fig. 2 illustrates that a ray $\bar{m}(t)$ is reflected from the paraboloid mirror at a point $y(t)$ on the mirror and captured by the orthographic projection camera as a point $p(t)$. Since $p(t)$ can be measured, the state $y(t)$ can be determined using (6) and (7). Since $\bar{m}(t)$ is related to $y(t)$ by (9), the state $y_4(t)$ must be estimated in order to estimate $\bar{m}(t)$. Therefore, the objective of the nonlinear observer is to estimate $y_4(t)$.

B. State Dynamics Formulation

The image dynamics for $y(t)$ and $y_4(t)$ can be determined by taking the time derivative of (4) and (8) and utilizing (3) and (5) as

$$\begin{aligned} \dot{y} &= f(y,a) + h(y,b) y_4, \\ \dot{y}_4 &= g(y, y_4, b, a_{ij}). \end{aligned} \tag{10}$$

In (10), the auxiliary function $f(y,a) = \begin{bmatrix} f_1 & f_2 & f_3 \end{bmatrix}^T \in \mathbb{R}^3$ is defined as

$$f \triangleq \begin{bmatrix} \sum_{i=1}^3 \left(a_{1i} y_i + \frac{y_1}{2\lambda}(a_{3i} y_i) - \frac{y_1}{2\lambda(2\lambda + y_3)} \beta_i \right) \\ \sum_{i=1}^3 \left(a_{2i} y_i + \frac{y_2}{2\lambda}(a_{3i} y_i) - \frac{y_2}{2\lambda(2\lambda + y_3)} \beta_i \right) \\ \sum_{i=1}^3 \left(a_{3i} y_i + \frac{y_3}{2\lambda}(a_{3i} y_i) - \frac{y_3}{2\lambda(2\lambda + y_3)} \beta_i \right) \end{bmatrix} \tag{11}$$

where $\beta_i \in \mathbb{R}$ is defined as

$$\beta_i \triangleq a_{1i} y_1 y_i + a_{2i} y_2 y_i + a_{3i} y_3 y_i, \tag{12}$$

$h(y,b) = \begin{bmatrix} h_1 & h_2 & h_3 \end{bmatrix}^T \in \mathbb{R}^3$ is defined as

$$h \triangleq \begin{bmatrix} b_1 - \frac{y_1^2 b_1}{2\lambda(2\lambda+y_3)} - \frac{y_1 y_2 b_2}{2\lambda(2\lambda+y_3)} - \frac{y_1 y_3 b_3}{2\lambda(2\lambda+y_3)} + \frac{b_3 y_1}{2\lambda} \\ b_2 - \frac{y_1 y_2 b_1}{2\lambda(2\lambda+y_3)} - \frac{y_2^2 b_2}{2\lambda(2\lambda+y_3)} - \frac{y_2 y_3 b_3}{2\lambda(2\lambda+y_3)} + \frac{b_3 y_2}{2\lambda} \\ b_3 - \frac{y_1 y_3 b_1}{2\lambda(2\lambda+y_3)} - \frac{y_2 y_3 b_2}{2\lambda(2\lambda+y_3)} - \frac{y_3^2 b_3}{2\lambda(2\lambda+y_3)} + \frac{b_3 y_3}{2\lambda} \end{bmatrix}, \tag{13}$$

and the nonlinear function $g(y, y_4, b, a) \in \mathbb{R}$ is defined as

$$\begin{aligned} g &= \frac{y_4}{2\lambda} \sum_{i=1}^3 a_{3i} y_i - \frac{y_4}{2\lambda(2\lambda + y_3)} \sum_{i=1}^3 \beta_i \\ &\quad - \frac{1}{2\lambda(2\lambda + y_3)} \left(\sum_{i=1}^3 y_i b_i - b_3(2\lambda + y_3) \right) y_4^2. \end{aligned} \tag{14}$$

Based on the structure of (14), $g(y, y_4, b, a)$ is locally Lipschitz with respect to the second argument as

$$g(y, y_4, b, a) - g(y, \hat{y}_4, b, a) = \Lambda (y_4 - \hat{y}_4)$$

where $\Lambda \in \mathbb{R}$ is a Lipschitz constant.

Assumption 5: The normed square of $h(y,b)$ in (13) is assumed to be non-zero $\forall t \geq 0$. This is an observability condition for (10)–(14). The observability condition physically means that camera must translate in at least one of the three directions and should not travel parallel to $y(t)$[1].

C. Nonlinear SfM Observer

In this section, a nonlinear SfM estimator is presented for the dynamic system given by (10)-(14) assuming that all of the motion parameters, i.e. $b(t)$ and $a_{ij}(t)$, of the moving camera are known. Scenarios where the relative motion parameters are known include a camera attached to the end-effector of a robot or attached to a vehicle with known motion acquired from a GPS, an IMU, or other sensor data.

[1]If camera travels parallel to vector $y(t)$ then the observation of the point does not change in the image.

1) Observer Design: The subsequent development is based on the strategy of developing observers for both the measurable states $y(t)$ and the unmeasurable state $y_4(t)$. A composite error $e(t) = \begin{bmatrix} e_1 & e_2 & e_3 & e_4 \end{bmatrix}^T \in \mathbb{R}^4$ is used to quantify the observer objective as

$$e \triangleq \begin{bmatrix} y_1 - \hat{y}_1 & y_2 - \hat{y}_2 & y_3 - \hat{y}_3 & y_4 - \hat{y}_4 \end{bmatrix}^T. \quad (15)$$

Based on the coupled form of (10) and the subsequent stability analysis, the estimates $\hat{y}_i(t) \in \mathbb{R}\ \forall i = 1,2,3,4$ are updated according to

$$\dot{\hat{y}}_i = f_i(y, a_{ij}, b_k) + h_i(y,b)\hat{y}_4 + K_{ii}e_i \qquad \forall i = 1,2,3 \quad (16)$$

where $K_{ii} \in \mathbb{R}$ are the diagonal elements of the positive-definite matrix $K \in \mathbb{R}^{3\times 3}$, and $\hat{y}_4(t)$ is generated based on the locally Lipschitz smooth projection defined as [31]

$$\dot{\hat{y}}_4(t) = proj(\hat{y}_4, \phi) = \begin{cases} \phi & \text{if } \underline{y_4} \le \hat{y}_4(t) \le \bar{y}_4 \text{ or} \\ & \text{if } \hat{y}_4(t) > \bar{y}_4 \text{ and } \phi(t) \le 0 \text{ or} \\ & \text{if } \hat{y}_4(t) < \underline{y_4} \text{ and } \phi(t) \ge 0 \\ \bar{\phi} & \text{if } \hat{y}_4(t) > \bar{y}_4 \text{ and } \phi(t) > 0 \\ \breve{\phi} & \text{if } \hat{y}_4(t) < \underline{y_4} \text{ and } \phi(t) < 0 \end{cases} \quad (17)$$

where $\phi(y, \hat{y}_4, a_{ij}, b, e, \dot{e}) \in \mathbb{R}$ is defined as[2]

$$\phi \triangleq g(y, \hat{y}_4, b, a_{ij}) + \sum_{i=1}^{3} h_i e_i + k_s \frac{\sum_{i=1}^{3} h_i(\dot{e}_i + K_{ii}e_i)}{\|h\|^2} \quad (18)$$

where $k_s(t)$ is an estimator gain and $\bar{\phi}(y, \hat{y}_4, a_{ij}, b, e, \dot{e}, \delta) \in \mathbb{R}$ and $\breve{\phi}(y, \hat{y}_4, a_{ij}, b, e, \dot{e}, \delta) \in \mathbb{R}$ are defined as

$$\bar{\phi} \triangleq \left[1 + \frac{\bar{y}_4 - \hat{y}_4}{\delta}\right]\phi, \quad \breve{\phi} \triangleq \left[1 + \frac{\hat{y}_4 - \underline{y_4}}{\delta}\right]\phi. \quad (19)$$

The projection in (17) ensures that the estimate $\hat{y}_4 \in \Omega_\delta$ $\forall t \ge 0$, where

$$\Omega_\delta = \{q \mid \underline{y_4} - \delta \le q \le \bar{y}_4 + \delta\}$$

for some known arbitrary constant $\delta > 0$. In (18), an estimator gain $k_s(t) \in \mathbb{R}$ is selected as

$$k_s(t) \ge \frac{1}{2\lambda}\sum_{i=1}^{3} a_{3i}y_i - \frac{1}{2\lambda(2\lambda + y_3)}\sum_{i=1}^{3}\beta_i + \left|\frac{1}{2\lambda(2\lambda + y_3)}\left(\sum_{i=1}^{3} y_i b_i - b_3(2\lambda + y_3)\right)\right| \cdot \bar{y}_4(1+\delta). \quad (20)$$

Remark 2: Since the state $y(t)$ is measurable, one way to choose initial conditions for the observer is

$$\hat{y}(t_0) = \begin{bmatrix} y_1(t_0) & y_2(t_0) & y_3(t_0) \end{bmatrix}^T, \quad \hat{y}_4(t_0) = y_{40} \quad (21)$$

[2]The observability condition in Assumption 5 ensures that $\|h(t)\|^2$ is non-zero.

where $y_{40} \in \mathbb{R}$ is an arbitrary constant. The choice of the initial conditions in (21) yields

$$e_1(t_0) = e_2(t_0) = e_3(t_0) = 0.$$

Remark 3: Since λ is small compared to $L(\bar{m})$, then $y_4(t)$ is a small number. Thus, the third term in (20) is a small number. The first and second term are exactly known. This fact allows the observer gain to be a small number which is an advantage of the proposed observer.

2) Error Dynamics: Differentiating (15) and using (10)-(13) and (16) yields

$$\dot{e}_i = h_i e_4 - K_{ii}e_i, \qquad \forall i = 1,2,3, \quad (22)$$

Using (22), $e_4(t)$ can be expressed as

$$e_4 = \frac{\sum_{i=1}^{3} h_i(\dot{e}_i + K_{ii}e_i)}{\|h\|^2}. \quad (23)$$

Since $\dot{\hat{y}}_4(t)$ is generated from a projection law, three possible cases for $\dot{e}_4(t)$ are considered.

Case I: $\underline{y_4} \le \hat{y}_4(t) \le \bar{y}_4$ or if $\hat{y}_4(t) > \bar{y}_4$ and $\phi(t) \le 0$ or if $\hat{y}_4(t) < \underline{y_4}$ and $\phi(t) \ge 0$: After using (10), (14), (17), (18), and (23), the time derivative of $e_4(t)$ in (15) can be determined as

$$\dot{e}_4 = \alpha \quad (24)$$

where $\alpha(y, y_4, \hat{y}_4, a_{ij}, b) \in \mathbb{R}$ is defined as

$$\alpha \triangleq \frac{e_4}{2\lambda}\sum_{i=1}^{3} a_{3i}y_i - \frac{e_4}{2\lambda(2\lambda + y_3)}\sum_{i=1}^{3}\beta_i - \sum_{i=1}^{3} h_i e_i - k_s e_4 - \frac{(y_4 + \hat{y}_4)e_4}{2\lambda(2\lambda + y_3)}\left(\sum_{i=1}^{3} y_i b_i - b_3(2\lambda + y_3)\right) \quad (25)$$

Case II: $\hat{y}_4(t) > \bar{y}_4$ and $\phi(t) > 0$: After using (10), (17), and the definition of $\bar{\phi}(t)$ given by (19), the time derivative of $e_4(t)$ in (15) can be determined as

$$\dot{e}_4 = \dot{y}_4 - \phi - \frac{\bar{y}_4 - \hat{y}_4}{\delta}\phi = \alpha - \frac{\bar{y}_4 - \hat{y}_4}{\delta}\phi. \quad (26)$$

Case III: $\hat{y}_4(t) < \underline{y_4}$ and $\phi(t) < 0$: After using (10), (17), and the definition of $\breve{\phi}(t)$ given by (19), the time derivative of $e_4(t)$ in (15) can be determined as

$$\dot{e}_4 = \dot{y}_4 - \phi - \frac{\hat{y}_4 - \underline{y_4}}{\delta}\phi = \alpha - \frac{\hat{y}_4 - \underline{y_4}}{\delta}\phi. \quad (27)$$

3) Stability Analysis: The stability of the proposed observer is analyzed using a Lyapunov-based approach. Since, the observer uses a projection law, the stability is examined for all three cases of the projection.

Theorem: The observer in (16)–(19) is exponentially stable provided Assumptions 1–5 are satisfied, and $k_s(t)$ is selected according to (20).

Proof: Consider the domain $\mathcal{D} \subset \mathbb{R}^4$ containing $e(0)$ and a continuously differentiable, radially unbounded Lyapunov function, $V(e,t) : \mathcal{D} \times [0,\infty) \to \mathbb{R}^+$, defined as

$$V \triangleq \frac{1}{2}e^T e. \quad (28)$$

Case I: $\underline{y_4} \leq \hat{y}_4(t) \leq \bar{y}_4$ or if $\hat{y}_4(t) > \bar{y}_4$ and $\phi(t) \leq 0$ or if $\hat{y}_4(t) < \underline{y_4}$ and $\phi(t) \geq 0$: Taking the derivative of $V(e)$ and utilizing (22) and (24) yields

$$\begin{aligned}\dot{V} &= \sum_{i=1}^{3} e_i(h_i e_4 - K_{ii} e_i) \\ &+ e_4 \left(\frac{e_4}{2\lambda} \sum_{i=1}^{3} a_{3i} y_i - \frac{e_4}{2\lambda(2\lambda + y_3)} \sum_{i=1}^{3} \beta_i \right. \\ &- \frac{e_4(y_4 + \hat{y}_4)}{2\lambda(2\lambda + y_3)} \left(\sum_{i=1}^{3} y_i b_i - b_3(2\lambda + y_3) \right) \\ &\left. - k_s e_4 - \sum_{i=1}^{3} h_i e_i \right). \end{aligned} \tag{29}$$

By choosing the gain $k_s(t)$ according to (20), the expression for $\dot{V}(t)$ can be upper bounded as

$$\dot{V} \leq -\sum_{i=1}^{3} K_{ii} e_i^2 - k_4 e_4^2$$

where $k_4 \in \mathbb{R}$ is a strictly positive number. Thus,

$$\dot{V} \leq -2 \min(K_{11}, K_{22}, K_{33}, k_4) V. \tag{30}$$

Using the Gronwall-Bellman lemma [32] yields

$$\|e(t)\| \leq \|e(t_0)\| \exp(-\min(k_{11}, k_{22}, k_{33}, k_4)t). \tag{31}$$

Case II: $\hat{y}_4(t) > \bar{y}_4$ and $\phi(t) > 0$: Taking the derivative of $V(e)$ and utilizing (22) and (26) yields

$$\dot{V} = \sum_{i=1}^{3} \left(-K_{ii} e_i^2 + h_i e_i e_4 \right) + e_4 \alpha - \left[e_4 \frac{\bar{y}_4 - \hat{y}_4}{\delta} \phi \right]. \tag{32}$$

Since $\frac{\bar{y}_4 - \hat{y}_4}{\delta} < 0$, $\phi(t) > 0$, and $e_4(t) < 0$, the bracketed term in (32) is positive, and (32) can be upper bounded as

$$\dot{V} \leq \sum_{i=1}^{3} \left(-K_{ii} e_i^2 + h_i e_i e_4 \right) + e_4 \alpha. \tag{33}$$

By substituting term α from (25) in (33) yields

$$\begin{aligned}\dot{V} &\leq \sum_{i=1}^{3} (-K_{ii} e_i + h_i e_i e_4) \\ &+ e_4 \left(\frac{e_4}{2\lambda} \sum_{i=1}^{3} a_{3i} y_i - \frac{e_4}{2\lambda(2\lambda + y_3)} \sum_{i=1}^{3} \beta_i \right. \\ &- \frac{(y_4 + \hat{y}_4) e_4}{2\lambda(2\lambda + y_3)} \left(\sum_{i=1}^{3} y_i b_i - b_3(2\lambda + y_3) \right) \\ &\left. - k_s e_4 - \sum_{i=1}^{3} h_i e_i \right). \end{aligned}$$

By choosing the gain $k_s(t)$ according to (20), the expression in (31) can be obtained.

Case III: $\hat{y}_4(t) < \underline{y_4}$ and $\phi(t) < 0$: Taking the derivative of $V(e)$ and utilizing (22) and (27) yields

$$\dot{V} = \sum_{i=1}^{3} \left(-K_{ii} e_i^2 + h_i e_i e_4 \right) + e_4 \alpha - \left[e_4 \frac{\hat{y}_4 - \underline{y_4}}{\delta} \phi \right]. \tag{34}$$

Since $\frac{\hat{y}_4 - \underline{y_4}}{\delta} < 0$, $\phi(t) < 0$, and $e_4(t) > 0$, the bracketed term in (34) is positive, and (34) can be upper bounded as in (33). By choosing the gain $k_s(t)$ according to (20), the expression in (31) can be obtained.

The expression in (31) shows that $e(t)$ is exponentially stable. Since $e(t) \in \mathcal{L}_\infty$, and $y(t)$, $y_4(t) \in \mathcal{L}_\infty$ from Assumption 4 and Remark 1, then $\hat{y}(t)$, $\hat{y}_4(t) \in \mathcal{L}_\infty$.

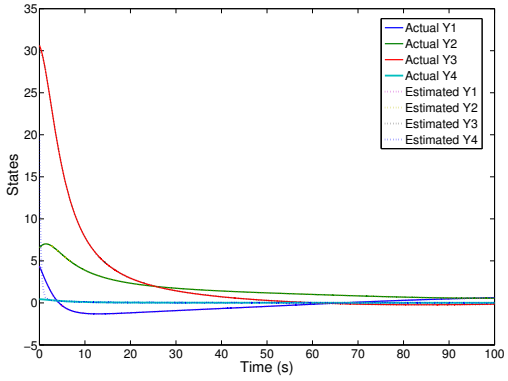

Fig. 3. Comparison of actual and estimated states with input noise.

Assumption 1 and 4 indicate that $y(t)$, $y_4(t)$, $b(t)$, $a_{ij}(t) \in \mathcal{L}_\infty$, thus (20) can be used to prove that $k_s(t)$ is bounded. Based on the fact that $y(t)$, $y_4(t)$, $e(t)$, $b(t)$, $a_{ij}(t) \in \mathcal{L}_\infty$, (22) and (24) can be used to show that $\dot{e}(t) \in \mathcal{L}_\infty$. Since $y_4(t)$ is estimated exponentially fast, (9) can be used to estimated $\bar{m}(t)$ exponentially fast.

V. Simulations

A numerical simulation is presented to illustrate the performance of the proposed nonlinear observer. The simulation is performed for a paracatadioptric camera viewing a single stationary point. The camera is moving with the affine motion dynamics given by

$$\dot{\bar{m}} = \begin{bmatrix} -0.2 & 0.4 & -0.6 \\ 0.1 & -0.2 & 0.3 \\ 0.3 & -0.4 & 0.4 \end{bmatrix} \bar{m} + \begin{bmatrix} 0.2 \\ 0.25 \\ 0.2 \end{bmatrix}$$

with $\lambda = 0.5$ and the initial Euclidean coordinates

$$\bar{m}(t_0) = \begin{bmatrix} 10 & 15 & 50 \end{bmatrix}^T.$$

The initial conditions of the observer states are selected as

$$\hat{y}(t_0) = \begin{bmatrix} 10 & 10 & 10 \end{bmatrix}^T, \quad \hat{y}_4(t_0) = 10.$$

The input of the observer, measured using various sensors, is corrupted by white Gaussian noise to simulate experimental data. The signals measurable by the camera, i.e., $y_1(t), y_2(t)$ and the motion parameters measured by other sensors, i.e. $b(t)$, $a_{ij}(t)$ are subjected to additive white Gaussian noise using the AWGN function in Matlab, with a signal to noise ratio (SNR) of 50. The comparison of actual states $y(t), y_4(t)$ and estimated states $\hat{y}(t), \hat{y}_4(t)$ is shown in Fig. 3.

The estimated signal $y_4(t)$ is used to scale the state $y(t)$ to determine the 3D coordinates of the point, i.e. $\bar{m}(t)$. With the input noise, the estimated state $\hat{y}_4(t)$ is also noisy. Thus, it is filtered using a low pass filter and then used to scale the state $y(t)$ to determine $\bar{m}(t)$. The comparison of actual $\bar{m}(t)$ and estimated $\bar{m}(t)$ is depicted in Figure 4. The error in the estimation of $y_4(t)$ is within $\pm 1\%$, despite the noisy input data from the sensors and the observer estimated the 3D coordinates of the points successfully.

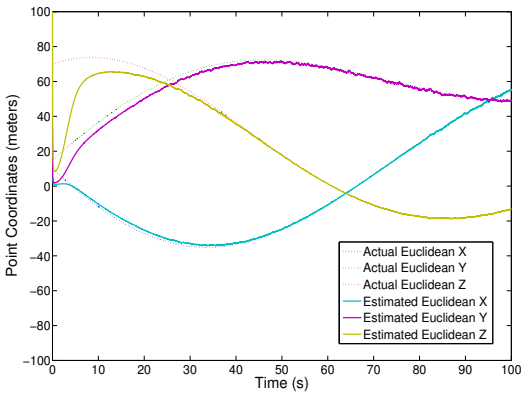

Fig. 4. Comparison of actual and estimated 3D Euclidean coordinates of a point with input noise.

VI. Conclusion

In this paper, an nonlinear observer is presented for estimating the structure of an object viewed by a moving paracatadioptric camera. The observer is analytically proven to exponentially converge provided a developed observability condition is satisfied. Performance of the observer is tested in simulation in the presence of input noise. Good convergence is obtained despite noisy image and motion parameter data. Future efforts will focus on testing the observer with experimental data.

References

[1] F. Kahl and R. Hartley, "Multiple-view geometry under the l_∞ -norm," *IEEE Transactions on Patterm Analysis and Machine Intelligence*, vol. 30, no. 9, pp. 1603–1617, Sept. 2008.

[2] S. Soatto and P. Perona, "Reducing structure from motion: A general framework for dynamic vision, part 1: Modeling," *IEEE Transactions on Pattern Analysis and Machine Intelligence*, vol. 20, no. 9, 1998.

[3] A. Azarbayejani and A. P. Pentland, "Recursive estimation of motion, structure, and focal length," *IEEE Transactions on Pattern Analysis and Machine Intelligence*, vol. 17, no. 6, pp. 562–575, 1995.

[4] W. E. Dixon, Y. Fang, D. M. Dawson, and T. J. Flynn, "Range identification for perspective vision systems," *IEEE Trans. Automat. Contr.*, vol. 48, no. 12, pp. 2232–2238, 2003.

[5] G. Quian and R. Chellappa, "Structure from motion using sequential monte carlo methods," *International Journal of Computer Vision*, vol. 59, pp. 5–31, 2004.

[6] M. Jankovic and B. Ghosh, "Visually guided ranging from observations points, lines and curves via an identifier based nonlinear observer," *Systems and Control Letters*, vol. 25, no. 1, pp. 63–73, 1995.

[7] L. Matthies, T. Kanade, and R. Szeliski, "Kalman filter-based algorithms for estimating depth from image sequences," *Int. J. Computer Vision*, vol. 3, pp. 209–236, 1989.

[8] D. Karagiannis and A. Astolfi, "A new solution to the problem range identification in perspective vision systems," *IEEE Trans. Automat. Contr.*, vol. 50, pp. 2074–2077, 2005.

[9] Y. Ma, S. Soatto, J. Kosecká, and S. Sastry, *An Invitation to 3-D Vision*. Springer, 2004.

[10] S. Soatto, "3d structure from visual motion: Modeling, representation and observability," *Automatica*, vol. 33, no. 7, pp. 1287–1312, 1997.

[11] S. Soatto, R. Frezza, and P. Perona, "Motion estimation via dynamic vision," *IEEE Trans. Automat. Contr.*, vol. 41, no. 3, pp. 393–413, 1996.

[12] H. Kano, B. K. Ghosh, and H. Kanai, "Single camera based motion and shape estimation using extended kalman filtering," *Mathematical and Computer Modelling*, vol. 34, pp. 511–525, 2001.

[13] A. Chiuso, P. Favaro, H. Jin, and S. Soatto, "Structure from motion causally integrated over time," *IEEE Trans. Pattern Anal. Machine Intell.*, vol. 24, no. 4, pp. 523–535, 2002.

[14] X. Chen and H. Kano, "State observer for a class of nonlinear systems and its application to machine vision," *IEEE Trans. Automat. Contr.*, vol. 49, no. 11, pp. 2085–2091, Nov 2004.

[15] S. Baker and S. Nayar, "A theory of single-viewpoint catadioptric image formation," *International Journal of Computer Vision*, vol. 35, no. 2, pp. 175–196, 1999.

[16] C. Geyer and K. Daniilidis, "Catadioptric projective geometry," *International Journal of Computer Vision*, vol. 45, no. 3, pp. 223–243, 2001.

[17] ——, "A unifying theory for central panoramic systems and practical implications," in *European Conference on Computer Vision*, vol. 29. Springer, 2000, pp. 159–179.

[18] S. Nayar, "Catadioptric omnidirectional camera," in *IEEE Conference on Computer Vision and Pattern Recognition*, 1997, pp. 482–488.

[19] B. Micusik and T. Pajdla, "Structure from motion with wide cicular field of view cameras," *IEEE Trans. Pattern Anal. Machine Intell.*, vol. 28, no. 7, pp. 1135–1149, July 2006.

[20] M. Lhuillier, "Toward flexible 3d modeling using a catadioptric camera," in *IEEE Conference on Computer Vision and Pattern Recognition*, 2007, pp. 1–8.

[21] ——, "Automatic scene structure and camera motion using a catadioptric system," *Computer Vision and Image Understanding*, vol. 109, no. 2, pp. 186–203, 2008.

[22] C. Geyer and K. Daniilidis, "Structure and motion from uncalibrated catadioptric views," in *IEEE Conference on Computer Vision and Pattern Recognition*, vol. 1, 2001.

[23] ——, "Mirrors in motion: Epipolar geometry and motion estimation," in *IEEE International Conference on Computer Vision*, 2003, pp. 766–773.

[24] B. Micusik and T. Pajdla, "Autocalibration and 3d reconstruction with non-central catadioptric cameras," in *IEEE conference on Computer Vision and Pattern Recognition*, 2004, pp. 58–65.

[25] L. Ma, Y. Chen, and K. L. Moore, "Range identification for perspective dynamic systems with 3D imaging surfaces," in *Proc. American Control Conference*, 2005, pp. 3671–3675.

[26] S. Gupta, D. Aiken, G. Hu, and W. E. Dixon, "Lyapunov-based range and motion identification for a nonaffine perspective dynamic system," in *Proc. American Control Conference*, 2006, pp. 4471–4476.

[27] C. Geyer and K. Daniilidis, "Paracatadioptric camera calibration," *IEEE Transactions on Pattern Analysis and Machine Intelligence*, pp. 687–695, 2002.

[28] G. Hu, D. Aiken, S. Gupta, and W. Dixon, "Lyapunov-Based Range Identification For Paracatadioptric Systems," *IEEE Transactions on Automatic Control*, vol. 53, no. 7, pp. 1775–1781, 2008.

[29] S. Hutchinson, G. Hager, and P. Corke, "A tutorial on visual servo control," *IEEE Trans. Robot. Automat.*, vol. 12, no. 5, pp. 651–670, Oct. 1996.

[30] R. Y. Tsai and T. S. Huang, "Estimating three-dimensional motion parameters of a rigid planar patch," *IEEE Transactions on Acoustics, Speech, Signal Processing*, vol. ASSP-29, no. 6, pp. 1147–1152, 1981.

[31] H. Khalil, "Adaptive Output Feedback Control of Nonlinear Systems Represented by Input-Output Models," *IEEE Transactions on Automatic Control*, vol. 41, no. 2, p. 177, 1996.

[32] C. Chicone, *Ordinary Differential Equations with Applications*, 2nd ed. Springer, 2006.